

ChemComm

Accepted Manuscript



This article can be cited before page numbers have been issued, to do this please use: Y. Dong, Y. Li, X. Zhao, H. Yin, G. Chen and S. Yang, *Chem. Commun.*, 2016, DOI: 10.1039/C6CC07321B.



This is an Accepted Manuscript, which has been through the Royal Society of Chemistry peer review process and has been accepted for publication.

Accepted Manuscripts are published online shortly after acceptance, before technical editing, formatting and proof reading. Using this free service, authors can make their results available to the community, in citable form, before we publish the edited article. We will replace this Accepted Manuscript with the edited and formatted Advance Article as soon as it is available.

You can find more information about Accepted Manuscripts in the [author guidelines](#).

Please note that technical editing may introduce minor changes to the text and/or graphics, which may alter content. The journal's standard [Terms & Conditions](#) and the ethical guidelines, outlined in our [author and reviewer resource centre](#), still apply. In no event shall the Royal Society of Chemistry be held responsible for any errors or omissions in this Accepted Manuscript or any consequences arising from the use of any information it contains.



Journal Name

COMMUNICATION

Drug-loaded nanoscale metal-organic framework with tumor targeting agent for highly effective hepatoma therapy

Yan-An Li,^a Xiao-Dong Zhao,^{a,b} Hai-Peng Yin,^b Gong-Jun Chen,^a Song Yang,^a Yu-Bin Dong^{a*}Received 00th January 20xx,
Accepted 00th January 20xx

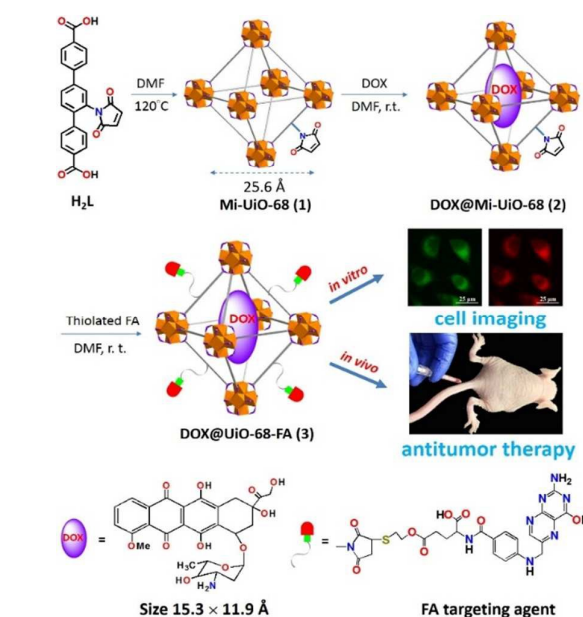
DOI: 10.1039/x0xx00000x

www.rsc.org/

Drug delivery systems with targeting agents for precise drug release in cancer therapy is very significant and important. Herein, we report rational design and synthesis of a DOX (doxorubicin) loaded UiO-68-type of nanoscale metal-organic framework (NMOF) with tumor targeting agent (folic acid, FA), DOX@UiO-68-FA (3), as a multifunctional drug delivery system for hepatoma (Hep G2) therapy via tail-vein injection. Compared to free DOX, FA-unloaded DOX@Mi-UiO-68 (2), 3 exhibits a much higher antitumor efficacy, which was confirmed by cell imaging, standard 3-(4,5)-dimethylthiazol-2-yl)-2,5-diphenyltetrazolium bromide (MTT) proliferation and *in vivo* experiments.

Nanoscale metal-organic frameworks (NMOFs), as a typical class of nano-sized porous hybrid material, provided a variety of attractive potential applications, including adsorption/separation, heterogeneous catalysis and sensing.^[1] Due to their nanoscale particle size, high surface area, large porosity, and low toxicity, NMOFs have been recently demonstrated to be the ideal platforms for drug upload and controlled delivery in medical application, especially cancer therapy.^[2]

It is known that the surface functionality of NMOFs can be covalently modified by virtue of post-synthetic approach.^[3] In principle, as drug carriers, NMOFs could be endowed targeting property towards specific tumor biosignals via purposefully functional decoration on the organic groups attached to organic linkers. In this way, targeting functionality, together with drug loading, delivery and medical treatment properties, could be logically integrated into a single NMOF platform, consequently,



Scheme 1. Design and fabrication of FA targeting agent decorated drug delivery system 3, and its application in cell imaging and *in vivo* antitumor therapy.

a higher efficient chemotherapy would be realized. So far, only a few examples of NMOF materials for *in vivo* cancer therapy, including photodynamic therapy (PDT) and drug delivery NMOF systems, have been reported. The targeting agent decorated NMOF drug delivery system, derived from the post-synthetic covalent modification, for cancer therapy via tail-vein injection, to our knowledge, is unprecedented.^[4] On the other hand, the targeting antitumor treatment base on drug delivery system *via* vein injection would be more significant potential for clinical translation.

In this contribution, we report a multifunctional integrated drug delivery system DOX@UiO-68-FA (3, DOX = doxorubicin, FA = folic acid) based on a UiO-68-type of NMOF *via* post-synthetic covalent modification (Scheme 1). It exhibits high efficient antitumor efficacy which is confirmed by cell imaging, MTT proliferation and *in vivo* experiments on Hep G2 subcutaneous xenograft murine model *via* tail-vein injection.

^a College of Chemistry, Chemical Engineering and Materials Science, Collaborative Innovation Center of Functionalized Probes for Chemical Imaging in Universities of Shandong, Key Laboratory of Molecular and Nano Probes, Ministry of Education, Shandong Normal University, Jinan 250014, P. R. China. E-mail: yubindong@sdu.edu.cn

^b Institute of Materia Medica, Shandong Academy of Medical Sciences, Jinan 250062, P. R. China.

Electronic Supplementary Information (ESI) available: Synthesis and additional characterization for ligand H₂L and 1-3, experimental details for DOX loading and release, cytotoxicity test, MTT, animal tumor xenograft models and *in vivo* anticancer test. See DOI: 10.1039/x0xx00000x

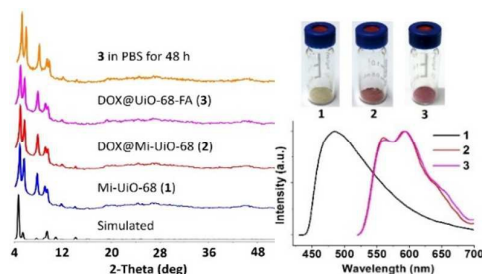


Fig. 1 Left: XRPD patterns of **1-3** and simulated XRPD pattern of UiO-68. Compared to **1**, there are no characteristic differences in the intensities in XRPD peaks of **2** and **3** after DOX loading and FA decoration because of the low included DOX and FA amount (ESI). Right: normalized solid-state emission spectra of **1-3**. Photographs of **1-3** samples are inserted.

We hypothesized that the UiO-68-based NMOF could be the ideal candidate for this multifunctional NMOF drug delivery system. First, UiO-68-type MOF is known to be very stable in aqueous media, and it possesses large internal pores (the distance between the opposite oxygen atoms in the larger octahedral SBUs pores is 25.6 \AA)⁵ which will facilitate relative larger sized drug molecule (for example DOX, dimension of $15.3 \times 11.9 \text{ \AA}$)²⁷ loading; second, UiO-type MOFs are low toxicity,²⁸ and their size can be readily scaled down to nanoregime ($< 200 \text{ nm}$),⁶ which is allowed it to be suitable for chemotherapy; third, the surface of UiO-type NMOFs can be covalently modified *via* post-synthesis with small molecular target agent FA, which is a widely recognized targeting agent for tumor cells.⁷

The preparation of nano-sized DOX@UiO-68-FA (**3**) was shown in Scheme 1. Its precursor of Mi-UiO-68 (**1**) was prepared by heating a DMF solution of the maleimide-attached H_2L ligand and ZrCl_4 at 120°C (ESI). The obtained Mi-UiO-68 MOF (**1**) was simply immersed in a DOX hydrochloride aqueous solution (1 mg/mL, 5 mL) at room temperature for 24 h (monitored by UV-vis spectra, ESI) to generate DOX@Mi-UiO-68 (**2**). SEM image and DLS measurement of **2** indicated that the NPs are centered at $140 \pm 21 \text{ nm}$ (ESI). After that, DOX@Mi-UiO-68 (**2**) was decorated by thiolated FA species (DMF, r. t.) *via* thiol-maleimide Michael-type addition⁸ to yield drug delivery system of DOX@UiO-68-FA (**3**) with the targeting agent (ESI).

The XRPD patterns of **1-3** are identical to that of pristine UiO-68,⁹ and thus indicated that the structural feature and crystallinity of UiO-68 framework were maintained during the DOX encapsulation and post-synthetic processes (Fig. 1). Furthermore, **3** is stable in cell culture fluid, making it suitable for application in cancer therapy (Fig. 1 and ESI). In addition, the encapsulated DOX emission¹⁰ was clearly detected in the solid state luminescent spectra of **2** and **3** ($\lambda_{\text{ex}} = 485 \text{ nm}$, $\lambda_{\text{em}} = 590 \text{ nm}$), which further confirmed this DOX encapsulation. Correspondingly, the colour of **1** changed from off-white to brown (**2**) and red-brown (**3**) (Fig. 1).

High resolution transmission electron microscopy (HR-TEM) and scanning electron microscope (SEM) showed that the obtained DOX@UiO-68-FA (**3**) nanoparticles are uniformly distributed (Fig. 2), which is further confirmed by the dynamic light scattering (DLS) measurement. As shown in Fig. 2, the hydrodynamic diameters of the DOX@UiO-68-FA (**3**) possess a

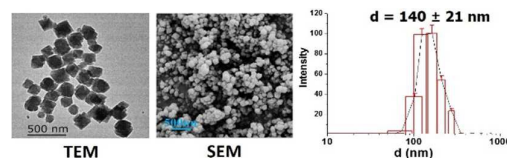


Fig. 2 Left: HR-TEM and SEM images of **3**. Right: dynamic light scattering (DLS) measurement of **3**.

narrow size distribution and the size of the NPs are centered at $140 \pm 21 \text{ nm}$. Such sized nanoparticles ($< 200 \text{ nm}$) definitely meet the requirement for tumor chemotherapy. Elemental analysis demonstrated that the post-synthetic FA decorating yield is ca. 4.2 mol % (ESI). For further confirmation this post-synthetic thiolated FA decoration, the reaction of the esterified maleimide-substituted organic linker H_2L with thiolated FA was examined before the synthesis of **3** under the same reaction conditions (DMF, r.t., 10 min.). The reaction readily proceeded and the expected thiolated FA decorated product was unambiguously confirmed by the MS spectrum (ESI). Compared to **2** (ESI), although no detectable changes were observed after FA decoration based on SEM and DLS measurement, the corresponding Zeta potential changed from $-15.7 (\pm 0.9) \text{ mV}$ (**2**) to $-13.5 (\pm 0.4) \text{ mV}$ (**3**).

The DOX loading amounts in **2** and **3** were determined by fluorescence spectroscopy to be 4.84 and 4.79 wt %, respectively (ESI).¹¹ When accounting for the involved FA (ca. 4.2 mol %) in **3**, the DOX content in **2** and **3** are basically the same, indicating that no DOX leaching occurred during the FA-decorated post-synthetic process.

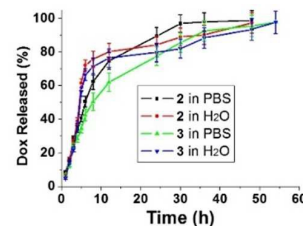


Fig. 3 DOX release profiles from DOX@Mi-UiO-68 (**2**) and DOX@UiO-68-FA (**3**) in PBS (pH = 7.4) and deionized aqueous solution (pH = 7.0) at 37°C , respectively. NMOF particles (1 mg) of **2** or **3** were uniformly dispersed in PBS (25 mL) and deionized water (25 mL) with shaking at 100 rpm. The fluorescent intensity ($\lambda_{\text{ex}} = 485 \text{ nm}$, $\lambda_{\text{em}} = 590 \text{ nm}$) of the DOX solution (1 mL each time) from above systems was measured at different time.

Next, we evaluated the DOX release at 37°C using either a cell culture fluid (phosphate buffered saline (PBS), 0.1 M at pH = 7.4) or deionized water.¹² As indicated in Fig. 3, the total amount of DOX in **2** and **3** was released in 40-50 and 50-55 h in both PBS and water media, respectively. So the complete drug release of **2** and **3** is faster in PBS than in water, which would be helpful for the *in vivo* anticancer application. In all case, release rate was fast over a first period of 12 h, and the release rate went down during the rest time. Compared to **2** (complete release at ca. 40 h) in PBS, DOX release from **3** is slightly slower (complete release at ca. 50 h), which is logically resulted from the blocking effect of the surface decorated FA species.

For examination of the cellular biocompatibility and membrane permeability of DOX@Mi-UiO-68 (**2**) and

DOX@UiO-68-FA (**3**), cell imaging experiments were carried out. Human hepatoma cells (Hep G2) and human hepatocyte (HL-7702) were selected and visualized by using a green channel for NMOFs ($\lambda_{\text{ex}} = 405 \text{ nm}$) and a red channel for DOX ($\lambda_{\text{ex}} = 485 \text{ nm}$). DOX@UiO-68-FA (**3**) and DOX@Mi-UiO-68 (**2**) nanocrystals were respectively incubated with Hep G2 cells for 2 h, and we notice that the both red ($\lambda_{\text{em}} = 560 - 610 \text{ nm}$) and green ($\lambda_{\text{em}} = 470 - 520 \text{ nm}$) luminescence are located in the cytoplasm, indicating that UiO-68 NMOFs with DOX is able to pass across the tumor cell membrane. Compared to DOX@UiO-68-FA (**3**, Fig. 4a), however, much fainter luminescence was observed in the case of Hep G2 incubated with DOX@Mi-UiO-68 (**2**) nanocrystals without FA targeting agent (Fig. 4b), which implies targeting ability of FA species in **3** is the key factor to affect the cellular uptake and cause this distinct difference in emission intensity, which is further well demonstrated by the flow cytometry analysis. As shown in Fig. 5, the mean fluorescence intensity (MFI) value in Hep G2 cells treated with **3** increased ca. 2.6-fold compared to that treated with **2**. In addition, when **2** and **3** were respectively incubated with normal liver cells of HL-7702 under the same conditions, no obvious fluorescence in either green or red channel was observed (Fig. 4c and 5), demonstrating the targeting agent FA-decorated NMOFs could be selectively enriched in Hepatocellular carcinoma cells (FR-positive) instead of normal liver cells (FR-negative). This is consistent with the fact that FA receptors such as FR α , FR β and FR γ are expressed at higher levels in many kinds of cancers, including liver cancer, to meet the FA demand of rapidly dividing cells under low FA conditions.⁷ On the other hand, when free Dox incubated with both Hep G2 and HL-7702, also no visual detectable red fluorescence for Dox was observed (Fig. 4), indicating MOF carrier is significantly important for Dox delivery.

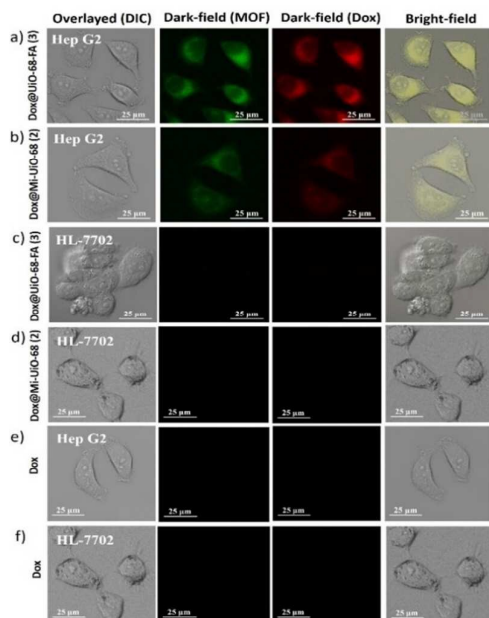


Fig. 4 Overlaid DIC confocal fluorescence image of living Hep G2 and HL-7702 cells. a-b) Hep G2 cells respectively incubated with DOX@UiO-68-FA (**3**, 10^{-3}

mg/mL) and DOX@Mi-UiO-68 (**2**, 10^{-4} mg/mL). c-d) HL-7702 incubated with DOX@UiO-68-FA (**3**, 10^{-4} mg/mL) and DOX@Mi-UiO-68 (**2**, 10^{-3} mg/mL). e-f) Hep G2 and HL-7702 respectively incubated with DOX. Incubation was carried out at 37°C under a humidified atmosphere containing 5% CO₂. Scale bars are 25 μm in all images.

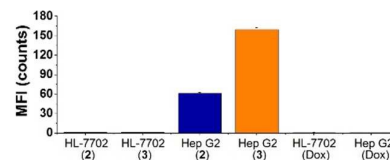


Fig. 5 The mean fluorescence intensity (MFI) of HL-7702 and Hep G2 cells treated by **2**, **3** and Dox, respectively ($P < 0.001$). The observation indicates that the binding of **3** to the Hep G2 cells is much stronger than that of **2**, which is clearly attributed to the high specific interaction between FA and Hep G2 cells. For comparison, HL-7702 cells only display very weak fluorescence in both green and red channels, suggesting a very low nonspecific binding of **2** to the cells. Dox incubated with both Hep G2 and HL-7702, also no visual detectable red fluorescence for Dox was observed, indicating Dox has bad penetration ability through cell membrane.

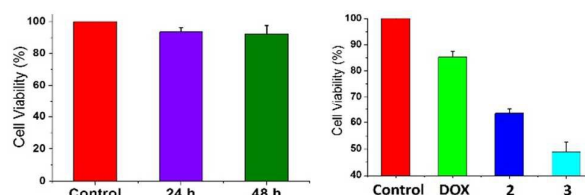


Fig. 6 MTT experiments for cell viability ($P < 0.005$). Left: control experiment and incubation of Hep G2 cells with DOX-unloaded **3** for 24 and 48 h. Right: control experiment and incubation of Hep G2 cells with free DOX, **2** and **3** for 48 h, respectively.

In addition, cell viabilities of DOX unloaded framework, free DOX, **2** and **3** was evaluated and the values were determined by the standard 3-(4,5)-dimethylthiazol-2-yl)-2,5-diphenyltetrazolium bromide (MTT) proliferation test at 37°C and 48 h incubation. As shown in Fig. 6, DOX unloaded NMOF (10^{-3} mg/mL) showed basically no cytotoxicity to Hep G2 cells, indicating that the inhibition effect of the DOX-unloaded UiO-68 framework is negligible (viability: 93.8% (24 h), 92.8% (48 h)). In addition, MTT experiments were also performed to test the cytotoxicity of free DOX, DOX@Mi-UiO-68 (**2**) and DOX@UiO-68-FA (**3**) toward Hep G2 cells. Fig. 6 shows that DOX@UiO-68-FA (**3**) exhibits the highest cytotoxicity to tumor cells among free DOX, DOX@Mi-UiO-68 (**2**) and DOX@UiO-68-FA (**3**). At the concentration of 4.84×10^{-5} mg/mL, the cellular viability treated by free DOX is 85.4 % after 48 h. After treatment with DOX@Mi-UiO-68 (**2**) and DOX@UiO-68-FA (**3**) at a concentration of 10^{-3} mg/mL (equivalent to a concentration of DOX of 4.84×10^{-5} mg/mL) for 48 h, the viability is 63.5 and 48.9 %, respectively (Fig. 6).

Encouraged by above observation, we performed *in vivo* anticancer test. Xenografts were established from cultured cells to evaluate the *in vivo* antitumor effect of **3**. Human HepG2 cells were suspended via trypsinization and collected by centrifugation (1500 rpm, 4 min) and approximately 5×10^6 HepG2 cells in Dulbecco's Modified Eagle Medium (DMEM, 100 μL) were subcutaneously injected into right of the nude mice. The tumor volume (V) was calculated as $V = L \times W^2/2$ by measuring the length (L is the longest diameter) and width (W is the shortest diameter). The relative tumor volumes were calculated for each sample as V_t/V_0 (V_0 was the original tumor

volume). The treatments were administrated when the tumor volume reach to about 150 mm³.

When the tumor volume reached to ca. 150 mm³, the tumor-bearing mice were weighed and randomly divided into 4 groups (6 mice each group). The mice were subjected with different treatments: PBS (50 μL) only, free DOX, DOX@Mi-UiO-68 (**2**)

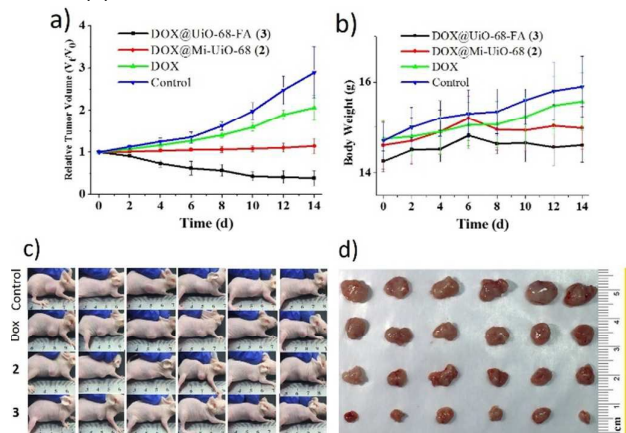


Fig. 7 *In vivo* anticancer test via tail-vein injection on Hep G2 tumor bearing mice ($P < 0.05$). a) Tumor volume after treatment. b) Corresponding mice weight after treatment. c) Photographs of mice on day 14. d) Photographs of corresponding excised tumors of each group after 14 days treatment. The Zr species was detected by ICP-MS after 48 h of injection, and biodistribution of **2** and **3** in mice organs after intravenous injection are given in ESI.

and DOX@UiO-68-FA (**3**) via tail-vein injection every two days intervals with the same dosage of 5 mg DOX/kg body weight. The tumor size and the body weight of each mouse were measured every two days intervals during two weeks.

As shown in Fig. 7, the relative tumor size follows a sequence of PBS > free DOX > **2** > **3** group, indicating that DOX-loaded **3** with targeting agent of FA exhibited the highest antitumor efficacy among free DOX, **2** and **3**. Fig. 7a shows that the mice tumor growth treated with PBS and free DOX could not be suppressed after 14 days, while the HepG2 proliferation treated with **2** was effectively inhibited which is reflected by the fact that almost no size expansion was detected in 14 days. In contrast, the tumor growth was significantly depressed by **3** and their size distinctly decreased. The corresponding size ratio compared to original tumor size is 2.90 (PBS), 2.06 (DOX), 1.14 (**2**) and 0.38 (**3**), respectively. As shown in Fig. 7b, the fast weight growth in PBS and DOX groups could be attributed to the aggressive tumor growth. The steady and slight body weight increase in **2** and **3** groups was observed after 14 days treatment, indicating their lower systemic toxicity and higher antitumor efficacy. Such observation was further supported by the excised tumors from the sacrificed mice (Fig. 7c and 7d).

In conclusion, we have designed and prepared a target agent bearing NMOF drug delivery system. The DOX loaded Mi-UiO-68 NMOF was covalently decorated by the targeting agent FA via thiol-maleimide Michael-type addition into this multifunctional drug delivery system. The cell imaging, MTT proliferation and *in vivo* studies demonstrated that the targeting FA-decorated DOX@UiO-68-FA exhibits the best therapeutic effect compared to free DOX and FA-undecorated DOX@Mi-UiO-68. This work demonstrates that drug loading,

release, targeting and medical treatment can be logically integrated into NMOF platform, which might be an alternative approach to access multifunctional cancer treatment system.

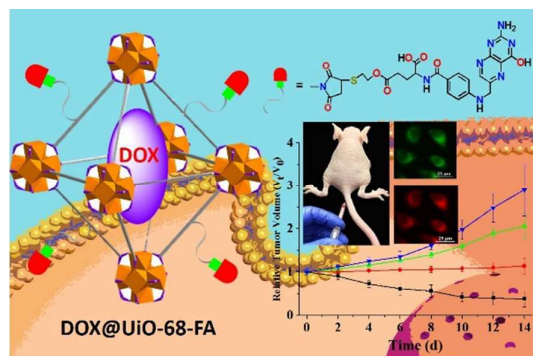
We are grateful for financial support from NSFC (Grant Nos. 21671122, 21475078 and 21271120), 973 Program (Grant Nos. 2013CB933800) and the Taishan scholar's construction project.

Notes and references

- (a) M. O'Keeffe, O. M. Yaghi, *Chem. Rev.*, 2012, **112**, 675-702. (b) J.-R. Li, J. Sculley, H.-C. Zhou, *Chem. Rev.*, 2012, **112**, 869-932. (c) Y. Cui, Y. Yue, G. Qian, B. Chen, *Chem. Rev.*, 2012, **112**, 1126-1162. (d) C. Wang, T. Zhang, W. Lin, *Chem. Rev.*, 2012, **112**, 1084-1104. (e) M. Yoon, R. Srirambalaji, K. Kim, *Chem. Rev.*, 2012, **112**, 1196-1231.
- (a) C. He, D. Liu, W. Lin, *Chem. Rev.*, 2015, **115**, 11079-11108. (b) P. Horcajada, R. Gref, T. Baati, P. K. Allan, G. Maurin, P. Couvreur, G. Férey, R. E. Morris, C. Serre, *Chem. Rev.*, 2012, **112**, 1232-1268. (c) E.-K. Lim, T. Kim, S. Paik, S. Haam, Y.-M. Huh, K. Lee, *Chem. Rev.*, 2015, **115**, 327-394. (d) Y. Tu, F. Peng, A. Adawy, Y. Men, L. K. E. A. Abdelmohsen, D. A. Wilson, *Chem. Rev.*, 2016, **116**, 2023-2078. (e) J. D. Rocca, D. Liu, W. Lin, *Acc. Chem. Res.*, 2011, **44**, 957-968. (f) P. Horcajada, T. Chalati, C. Serre, B. Gillet, C. Sebrie, T. Baati, J. F. Eubank, D. Heurtaux, P. Clayette, C. Kreuz, J.-S. Chang, Y. K. Hwang, V. Marsaud, P.-N. Bories, L. Cynober, S. Gil, G. Férey, P. Couvreur, R. Gref, *Nat. Mater.*, 2010, **9**, 172 - 178. (g) Á. Ruyra, A. Yazdi, J. Espin, A. Carné-Sánchez, N. Roher, J. Lorenzo, I. Imaz, D. Maspoch, *Chem. Eur. J.*, 2015, **21**, 2508-2518.
- (a) S. M. Cohen, *Chem. Rev.*, 2012, **112**, 970. (b) M. F. Lin, R. Matsuda, S. Kitagawa, *Chem. Mater.*, 2014, **26**, 310. (c) J. D. Evans, C. Sumbly, C. J. Doonan, *Chem. Soc. Rev.*, 2014, **43**, 5933-5951. (d) V. Valtchev, G. Majano, S. Mintova, J. Pérez-Ramírez, *Chem. Soc. Rev.*, 2013, **42**, 263-290.
- (a) K. Lu, C. He, W. Lin, *J. Am. Chem. Soc.*, 2014, **136**, 16712-16715. (b) K. Lu, C. He, W. Lin, *J. Am. Chem. Soc.*, 2015, **137**, 7600-7603. (c) M. Zheng, S. Liu, X. Guan, Z. Xie, *ACS Appl. Mater. Interfaces*, 2015, **7**, 22181-22187. (d) X.-G. Wang, Z.-Y. Dong, H. Cheng, S.-S. Wan, W.-H. Chen, M.-Z. Zou, J.-W. Huo, H.-X. Deng, X.-Z. Zhang, *Nanoscale*, 2015, **7**, 16061-16070.
- A. Schaate, P. Roy, A. Godt, J. Lippke, F. Waltz, M. Wiebacke, P. Behrens, *Chem. Eur. J.* 2011, **17**, 6643-6651.
- A. Schaate, P. Roy, A. Godt, J. Lippke, F. Waltz, M. Wiebacke, and P. Behrens, *Chem. Eur. J.*, 2011, **17**, 6643-6651.
- (a) C. Chen, J. Ke, X. E. Zhou, W. Yi, J. S. Brunzelle, J. Li, E.-L. Yong, H. E. Xu, K. Melcher, *Nature*, 2013, **500**, 486-489. (b) D. Peer, J. M. Karp, S. Hong, O. M. Farokhzad, R. Margalit, R. Langer, *Nat. Nanotechnol.*, 2007, **2**, 751-760. (c) M. J. Sailor, J.-H. Park, *Adv. Mater.*, 2012, **24**, 3779-3802. (d)
- Y.-A. Li, C.-H. Zhao, N.-X. Zhu, Q.-K. Liu, G.-J. Chen, J.-B. Liu, X.-D. Zhao, J.-P. Ma, S. Zhang, Y.-B. Dong, *Chem. Commun.* 2015, **51**, 17672-17675.
- J. H. Cavka, S. Jakobsen, U. Olsbye, N. Guillou, C. Lamberti, S. Bordiga, K. P. Lillerud, *J. Am. Chem. Soc.*, 2008, **130**, 13850-13851.
- D. K. Rana, S. Dhar, A. Sarkar, S. C. Bhattacharya, *J. Phys. Chem. A* 2011, **115**, 9169-9179.
- Y. Shen, E. Jin, B. Zhang, C. J. Murphy, M. Sui, J. Zhao, J. Wang, J. Tang, M. Fan, E. V. Kirk, W. J. Murdoch, *J. Am. Chem. Soc.* 2010, **132**, 4259-4265.
- H. Zheng, Y. Zhang, L. Liu, W. Wan, P. Guo, A. M. Nyström, X. Zou, *J. Am. Chem. Soc.*, 2016, **138**, 962-968.

Journal Name

COMMUNICATION



Drug loading, release, targeting and medical treatment are successfully integrated into a UiO-68-type NMOF platform via post-synthetic covalent modification, and the obtained DOX@UiO-68-FA can be a highly effective drug system for hepatoma therapy.